TOPOGRAPHIC RESPONSE OF NEARSHORE CURRENTS TO WIND: AN EMPIRICAL MODEL

By

T. J. Simons

National Water Research Institute

Canada Centre for Inland Waters

Burlington, Ontario, Canada L7R 4A6

NWRI UM NS #84-17

ABSTRACT

Observations of winds and currents along the northshore of Lake Ontario are analyzed to evaluate effects of topographic wave propagation on wind-driven currents. Lagged cross-correlations and spectral transfer fuctions between winds and currents are found to be consistent with the mechanism of resonant topographic wave response in the presence of bottom friction. Transfer function models in the time domain are shown to explain 70 to 80 percent of the variance of observed currents.

RÉSUMÉ

On analyse des observations des vents et des courants le long de la rive nord du lac Ontario afin d'évaluer les effets de la propagation des vagues topographiques sur les courants poussés par le vent. On constate que les corrélations croisées avec déphasage et les fonctions de transfert spectral entre vents et courants sont compatibles avec le mécanisme de résonnance des vagues topographiques en présence de friction sur le fond. On montre que des modèles des fonctions de transfert dans le temps expliquent de 70 à 80 pourcent de la variance des courants observés.

EXECUTIVE SUMMARY

The response of nearshore currents in large lakes to the forcing of the wind is the primary mechanism for transport and replacement of waters in this important zone. Models of this response have been advanced on the basis of a directly-forced and free response with resonance occurring at forcing frequencies.

A set of current observations in Lake Ontario during the homogeneous winter period of 1982/83 were obtained from an along-shore and cross-lake array of moored current meters. This set of data have permitted a comparison of modelled and measured responses and also the development of an empirical model of nearshore currents.

The observations are in essential agreement with the model. Amplitudes and phase lags are dependent upon resonant topographic response and bottom friction. The alongshore variation of phase lag demonstrates presence of topographic waves while a gradual shift of resonant frequency along the north shore is associated with shelf wave dispersion.

This set of data have provided an increased level of confidence in the prior numerical models and has also permitted the development of an empirical model. Thus, the understanding of the nearshore current responses to wind forcing during the homogeneous lake period is more founded.

RÉSUMÉ ADMINISTRATIF

Dans les grands lacs, la réponse des courants littoraux à l'action de force du vent est le principal mécanisme de transport et de remplacement de l'eau de cette importante zone. On a proposé des modèles de réponse, tant directement forcée que non forcée, la résonnance se produisant aux fréquences de force.

On a obtenu, à partir de courantomètres ancrés le long du littoral et en travers du lac Ontario, un ensemble d'observations des courants pour la période homogène de l'hiver de 1982-1983. Ces données ont permis de comparer les réponses mesurée et modélisée ainsi que de mettre au point un modèle empirique des courants littoraux.

Pour l'essentiel, les observations concordent avec le modèle. Les amplitudes et déphasages dépendent de la résonnance topographique et de la friction sur le fond. La variation du déphasage le long du littoral démontre la présence de vagues topographiques et un décalage graduel de la fréquence de résonnance le long de la rive nord est associé à la dispersion des vagues sur le plateau.

Cet ensemble de données a conféré un niveau de confiance accru aux modèles numériques antérieurs et a également permis la mise au point d'un modèle empirique. On comprend ainsi mieux les réponses des courants littoraux à l'action du vent pendant l'intervalle d'homogénéité du lac.

1 INTRODUCTION

In an earlier paper (Simons, 1983), hereafter referred to as RTR, it was argued that observed current fluctuations in homogeneous coastal waters cannot, in general, be explained by either a balance between local wind and bottom stress or by free topographic wave models. Calling to mind the familiar storm surge problem, the response of nearshore currents to wind was visualized as a combination of a directly-forced and a free response with resonance occurring at forcing frequencies corresponding to normal mode solutions. Using observations from Lake Ontairo it was also shown that for water depths less than 100 m, topographic waves are rapidly damped out by bottom friction and hence must be continually reinforced by new wind impulses.

The above study relied heavily on numerical models of shelves and rotating basins and to a much lesser extent on observations of winds and currents. The limited data base available for the study did not permit verification of some crucial model results such as the speed of alongshore wave propagation and alongshore variations in amplitude and resonance frequency of the current response. In the meantime, a more complete series of measurements have been made to test the validity of the earlier conclusions. These observations are reviewed in the present paper.

In the former paper it was also shown that the available current observations could be adequately simulated by dynamical models. Analysis and verification of model results in the frequency domain was based on the response of observed and computed currents to periodic wind forcing. Computations in the time domain were made by convolution of wind stress and impulse response functions obtained from two-dimensional numerical models. Naturally, linear transfer models in time can also be estimated directly from observed winds and currents. Such empirical models for nearshore currents are briefly explored in the last part of this paper.

2 TIME SERIES ANALYSIS

During the winter of 1982/83, extensive current measurements were made in Lake Ontario. The current meters were deployed in two arrays, the first one following the 50 m depth contour along the northshore, the second one extending across the lake from Port Hope, Ontario, to Point Breeze, New York (Fig. 1). Current meters were located at depths of 12 m below the surface and 1 m above the bottom and at a few intermediate depths in the cross-lake array. A total of 34 complete records were obtained for the 140-day period of measurement, 4 November 1982 to 23 March 1983.

The present analysis is concerned with the alongshore array and the northern part of the offshore array. The distance between stations and measurement depths are summarized in Table 1. Winds are available from routine weather observations at Toronto Island Airport, slightly to the west of current meter station A7. The stress is computed in the conventional manner with a drag coefficient of 1.2×10^{-3} for wind speeds less than 10 m s^{-1}, linearly increasing to 2.4×10^{-3} at speeds of 20 m s^{-1}, and equal to the latter value for higher wind speeds.

Energy spectra of currents showed that low frequency variations in all stations were aligned with the local bathymetry. From model experiments it is also known that current variations along the northshore of Lake Ontario are primarily induced by the alongshore component of the wind. Therefore, the following analysis deals with alongshore components of wind stress and currents.

An indication of topographic wave effects on the response of nearshore currents to wind is readily obtained by computing correlations between wind stress and current meter records at different time lags. Figure 2 shows lagged cross-covariances between the Toronto Island wind stress and all current observations in the nearshore zone. Solid curves represent surface measurements, dashed curves refer to bottom currents. Current reversals due to wave activity are evidenced by negative correlations starting three to five days after the wind. As expected, the directly-forced initial response to surface stress is considerably greater at the surface than at the bottom, but the subsequent free response is essentially uniform in the vertical. Unlike the cross-covariances, maximum cross-correlations are the same for surface and bottom currents since the standard deviations of the currents increase toward the surface.

The time lag of maximum correlation increases from the first to the last station of the alongshore array in agreement with the direction of shelf wave propagation. As discussed in RTR, Section 5, such an alongshore variation of phase lag between response and forcing occurs because a uniform wind blowing over a closed basin is equivalent to a wavelike wind pattern over a straight shelf. A much greater alongshore trend shows up in the time of zero-crossing of the correlation functions. This reflects the westward increase of dominant wave period along this shore found from shelf wave dispersion curves (RTR, Fig. 9) and confirmed by the following spectral results. However, as pointed out by a reviewer, a similar effect would result from wave propagation along a uniform shelf. While this cannot be overlooked, it is felt that the corresponding wave speed of 35 km/day would be an underestimate of the actual value.

The phase speed of shelf wave propagation may be estimated from lagged correlations between individual stations. Similar calculations have been made for the Oregon Shelf by Kundu and Allen

(1976) and for Lake Ontario by Clarke (1977) and Marmorino (1979). The results confirm that the time lags of maximum correlation between consecutive stations are in all cases consistent with westward wave propagation. The total lag between the first and last station is about 20 hrs, equivalent to a wave speed of 110 km/day. The speed estimates range from over 200 km/day for the central moorings to as low as 60 km/day for the western stations. This kind of variation might be expected from the above mentioned shelf wave dispersion curves but it should be recalled (RTR, Fig. 6) that the apparent phase propagation under conditions of periodic forcing may be significantly affected by friction.

3 SPECTRAL ANALYSIS

For a detailed analysis of the relation between wind and currents, recourse may be had to computations in the frequency domain. Of special interest is the spectral transfer function which represents the response of the current to periodic excitation by the wind. The spectral response function is the Fourier transform of the impulse response in the time domain (see, e.g., Blackman and Turkey, 1958). The latter is familiar from storm surge prediction (see, e.g., Schwab, 1979). The frequency response has an amplitude and a phase. The amplitude is the coherent part of the square root of the spectral energy ratio between currents and wind. The units are current ($m\ s^{-1}$) divided by wind stress ($N\ m^{-2}$). The phase follows from the cross-spectrum and is converted to the lag of the current behind the wind in units of the forcing period.

The power spectra and cross-spectra were computed by the lagged covariance method with maximum lag of 28 days, i.e., one fifth of the total record length of 140 days. Spectral estimates were obtained for periods equal to fractions of 56 days and smoothed by Hanning. Rotary spectra were also computed, showing that nearshore current oscillations were essentially rectilinear and oriented along local depth contours. As noted earlier, the cross-spectra between wind and currents were based on the alongshore components since the cross-shore component of the wind has less effect on currents in the coastal zone.

As expected from Fig. 2, the current meter spectra show smooth and consistent variations from one station to the next. It will suffice, therefore, to limit presentation of results to a few illustrations. The left pannel of Fig. 3 shows frequency response functions for the surface currents of the first, middle, and last station in the alongshore array. The right panel of Fig. 3 presents corresponding results for the first three cross-shore stations, including the cross-over station between alongshore and cross-shore arrays ($C_2 = A_3$). Coherences are shown at the top of Fig. 3. Amplitudes of bottom currents (not shown) are about one-third smaller than those at the surface, as anticipated from Fig. 2. The amplitude reduction between surface and bottom appears quite independent of frequency.

The observations of Fig. 3 may be compared with the model results presented in RTR. Amplitudes and phase lags are seen to display the characteristic frequency dependence of resonant topographic response in the presence of bottom friction. Without such topographic effects the amplitudes would increase more uniformly with period and the phase lags would vary much more slowly as a function of frequency (see, e.g., RTR, Fig. 15). In addition, the spectra confirm some model results which could not be verified in the earlier study due to sparsity of data. First of all, the alongshore variation of phase lag vividly demonstrates the presence of topographic waves. Secondly, it was anticipated that alongshore topographic variations and the associated shelf wave dispersion curves (RTR, Fig. 9) would cause a gradual shift in resonance frequency along Lake Ontario's northshore. This is indicated by the cross-covariances of Fig. 2 and it is amply confirmed by the spectral results of Fig. 3. Finally, numerical calculations for a circular basin (RTR, Fig. 6) suggested a counterclockwise shift of the maximum current response relative to the maximum alongshore component of the wind. This could account for the alongshore amplitude variations of the response functions shown in Fig. 3.

A few notes of caution must be added here. Results of model calculations (RTR, Fig. 3) suggest that alongshore variations of resonance frequencies due to alongshore depth variations are smaller than expected from local wave dispersion curves. This smoothing effect appears in the eastern half of the alongshore array (stations A1 to A4) but not in the western half (stations A4 to A7). Also, alongshore amplitude variations computed by the same model are not consistent with the present observations. Perhaps this effect of alongshore depth variation is obscured by the above mentioned counterclockwise shift of the current maximum or by variations in offshore distance. In any case, results from a two-dimensional numerical model of Lake Ontario show the same alongshore amplitude variations as found in the observed currents.

4 EMPIRICAL MODELS

While a spectral analysis of observations can provide useful insights into the dynamics of the nearshore zone, the more practical problem of modelling nearshore currents must be dealt with in the time domain. In view of the foregoing, the currents cannot be simulated adequately on the basis of a local balance between wind and bottom stress but must include effects of topographic wave propagation and hence, effects of forcing at distant locations. In principle, therefore, the model must cover the whole basin or shelf region. For a recent discussion of the basin-wide topographic response to wind, reference may be made to Schwab (1983). As long as the system is linear, however, it is always possible to compute impulse response functions for the location of interest. The local current is then obtained by convolution of the impulse response with the wind history in one or more stations.

In the previous paper (Simons, 1983), impulse response functions were computed from a two-dimensional numerical model of Lake Ontario. In addition to the linearity of the model, it was assumed that the scale of the forcing was sufficiently large compared to the size of the lake so that the forcing would be approximately uniform in space. It is clear that, given those assumptions and given local wind and current measurements, the impulse response may also be obtained directly from these observations. Just like the corresponding spectral transfer functions, empirical response functions in the time domain shed considerable light on the characteristic behavior of the system and, hence, provide a useful tool for verification of dynamic models. They can also, of course, be used for the practical purpose of modelling currents, thus eliminating the need for numerical models.

The impulse response in time is the Fourier transform of the frequency response function and *vice versa* (see, e.g., Blackman and Tukey, 1958). Since the latter are already available, the former can be readily obtained. The present spectral results were computed at frequency intervals of 1/56 cpd, the total number of frequency estimates being $28/\Delta t$, where Δt is the data interval in days. The corresponding Fourier transform has twice as many discrete values in time and is 56 days long. For practical purposes, this impulse response function may be severly truncated. The optimum length may be estimated by truncating the function at different points, convoluting the result with the wind record and comparing the computed current with the current meter record. This procedure showed that the error variance did not decrease if the response function was extended beyond 20 days. The corresponding error variances in percent of observed current variances are presented in Table 2(a).

The impulse response can also be obtained directly from time series of observed winds and currents by solving the system of equations generated by convolution of the unknown impulse response function with the wind history for each point of the current meter record. For reliable estimates, the data records should be much longer than the response function and hence the system of equations must be solved in a least squares sense. A number of such algorithms are available in standard computer libraries. Results for the present data set are presented in Table 2(b). Schwab (1979) used this method to obtain an empirical model for storm surge prediction and found the results comparable to those obtained from hydrodynamical models.

To illustrate the present results, Fig. 4 compares observed and computed currents for the same moorings as in Fig. 3. The data were smoothed by a low-pass filter with amplitude response decreasing from unity to zero between 24 and 18 hrs. The empirical model used for these calculations was obtained by the least squares method with data spacing of 12 hrs. As seen in Table 2, the error variances for these moorings range from 21 to 23 percent. It is evident that the errors tend to be correlated for all stations. This suggests that inaccurate wind stress estimates are the primary cause of discrepancies between observed and simulated currents. In addition, it should be noted that, although currents along Lake Ontario's north shore are primarily excited by alongshore wind impulses, some effects of cross-shore wind components will occur because the lake is a closed basin. The least squares algorithm can be readily extended to determine impulse responses for both wind components simultaneously. This procedure was found to reduce the mean squared error by up to one third but the results cannot be generalized since they are completely determined by the shape of the basin.

Since the response functions obtained from the data spectra were truncated and the least squares results were derived without regard to the spectra, the frequency transforms of these impulse response functions are not necessarily the same as the frequency response functions obtained from the data spectra (Fig. 3). To illustrate the consistency of the various calculations, Fig. 5 compares results for station A3. The solid line is the original frequency response shown by the solid line in the rhs of Fig. 3. The other two curves are the Fourier transforms of the empirical impulse response functions obtained by the two methods described above, the dashed line referring to the first method, the dotted line to the second. The empirical models tend to underestimate the energy transfer for periods of six to seven days and overestimate the low frequency energy.

As a final note it may be added that the impulse response function is an example of a general class of linear transfer models in the time domain. For other models of this type, reference may be made to Box and Jenkins (1970, Ch. 10). Such models are available in standard computer libraries and have also been used for storm surge prediction (Budgell and El-Shaarawi, 1979). Experiments along those lines were carried out here and indicated that these models might be preferable for single-step prediction with the past history of the current as well as the wind being known. For practical purposes, however, this is of less interest. If the Box-Jenkins models are reformulated in terms of the wind history alone, one obtains impulse response functions very similar to those discussed above.

5 SUMMARY AND CONCLUSIONS

In an earlier paper (Simons, 1983) hydrodynamic model results and a limited data set were analysed to evaluate effects of topographic wave propagation on wind-driven currents in homogeneous coastal waters. In the present paper a much more complete series of measurements made in the winter of 1982-1983 along the north shore of Lake Ontario were reviewed. Lagged cross-correlations and spectral transfer functions between winds and currents were found to be consistent with the mechanism of resonant topographic wave response damped by bottom friction. Alongshore variations of amplitude and resonance frequency of the current response reflected effects of alongshore topographic variations estimated from shelf wave dispersion curves.

Empirical transfer function models between wind and currents were also computed in the time domain. Impulse response functions were obtained as Fourier transforms of the frequency response functions and by a least squares fit of current records to wind history. Based on the alongshore component of the wind alone, these models were found to explain about 75 percent of the variance of observed currents.

ACKNOWLEDGEMENTS

J. Bull and C.R. Murthy planned the field program, W.M. Schertzer assisted in the data anlaysis, and A. El-Shaarawi and D.C.L. Lam provided advice on empirical model design.

REFERENCES

Blackman, R.B., and J.W. Tukey, 1958: The measurement of power spectra, Dover, New York, 190 pp.

Box, G.E.P., and G.M. Jenkins, 1970: Time series analysis: Forecasting and control. Holden-Day, San Francisco, 575 pp.

Budgell, W.P., and A. El-Shaarawi, 1979: Time series modelling of storm surges in a medium-sized lake. In Predictability and Modelling in Ocean Hydrodyn. (J.C.J. Nihoul, ed.), Elsevier Oceanogr. Ser. 25, 197-218.

Clarke, A.J., 1977: Observational and numerical evidence for wind-forced coastal trapped long waves. J. Phys. Oceanogr., 7, 231-247.

Kundu, P.K., and J.S. Allen, 1976: Some three-dimensional characteristics of low frequency current fluctuations near the Oregon coast. J. Geophys. Res., 84, 1206-1214.

Marmorino, G.O., 1979: Low-frequency current fluctuations in Lake Ontario, Winter 1972-1973. J. Geophys. Res., 84, 1206-1214.

Schwab, D.J., 1978: Simulation and forecasting of Lake Erie storm surges. Mon. Wea. Rev., 106, 1476-1487.

Schwab, D.J., 1979: Analytical and empirical response functions for storm surges on Lake Erie. Mar. Sci. Dir., Ottawa, Manuscript Rept. Ser. 53, 140-144.

Schwab, D.J., 1983: Numerical simulation of low-frequency current fluctuations in Lake Michigan. J. Phys. Oceanogr., 13, 2213-2224.

Simons, T.J., 1983: Resonant topographic response of nearshore currents to wind forcing. J. Phys. Oceanogr., 13, 512-523.

Table 1. Partial listing of current meter moorings in Lake Ontario, 4 November 1982 to 23 March 1983

Station	A1	A2	A3	A4	A5	A6	A7
Alongshore distance (km)	0	16	33	49	64	79	94
Sounding depth (m)	49	50	54	51	51	51	50
Depths of current meters (m)	12		12	12			12
	48	49		50	50	50	49

Station	C1	C2	C3	C4	C5	C6	C7
Offshore distance (km)	4	8	15	22	24	31	40
Sounding depth (m)	28	54	74	100	112	147	180
Depths of current meters (m)	12	12	12	12	12	12	12
			73	99	50	50	50
					111	146	179

Table 2. Error variance in percent of variance of observed current for (a) impulse response obtained from spectral response and (b) impulse response obtained by least squares fit

Station	A1	A2	A3	A4	A5	A6	A7	C1	C2	C3	C4
Depth											
12 m (a)	25		22	22			23	23	22	24	50
(b)	23		21	21			21	21	21	23	45
50 m (a)	30	21		22	25	26	26				
(b)	27	20		21	23	24	23				

FIGURE LEGENDS

Fig. 1: Current meter moorings in Lake Ontario, 4 November 1982 to 23 March 1983.

Fig. 2: Lagged cross-covariances between alongshore components of wind stress and currents

Fig. 3: Amplitude and phase of frequency response and coherence between wind stress and selected currents.

Fig. 4: Observed (solid) and computed (dashed) surface currents, smoothed by low-pass filter.

Fig. 5: Amplitude and phase of frequency response of current meter station A3. Solid curve: based on spectra of observed wind and current as in Fig. 3; dashed: Fourier transform of truncated impulse response obtained from spectra; dotted: Fourier transform of impulse response obtained from least squares fit.

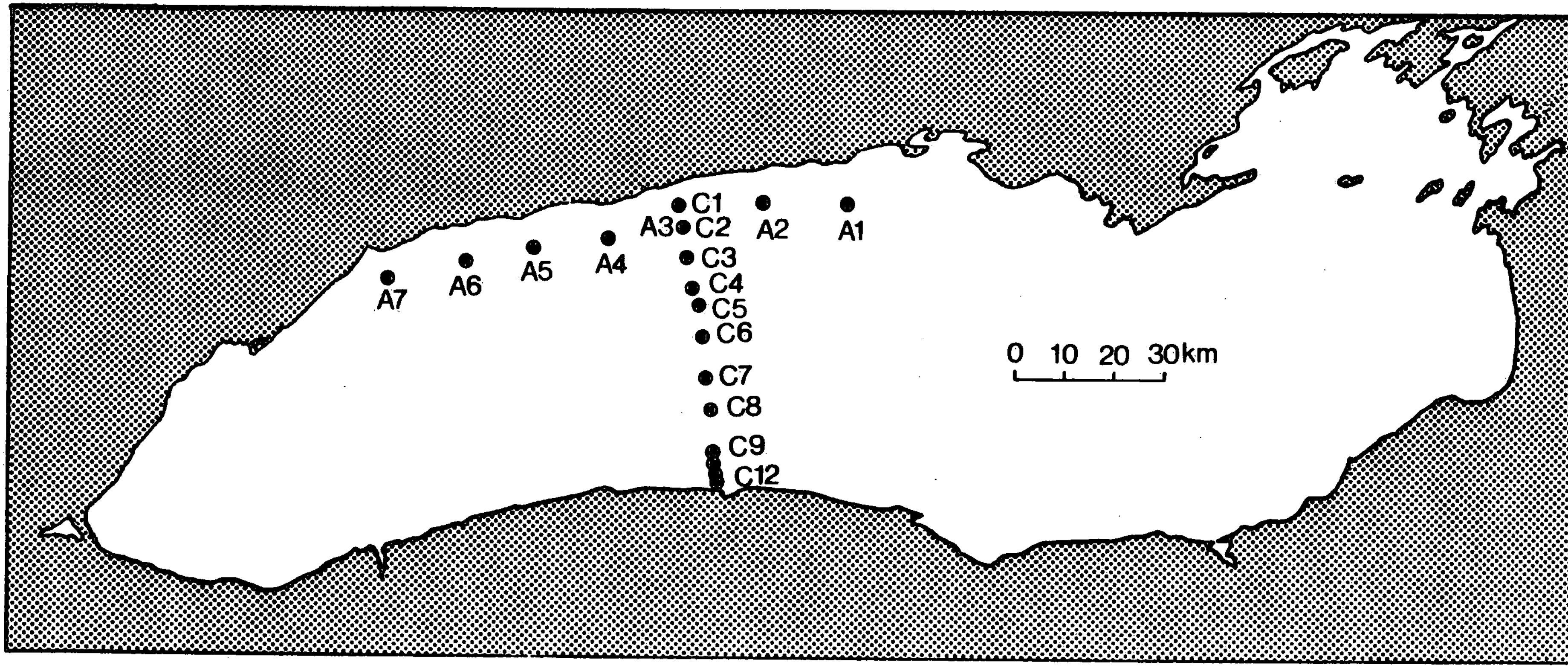
C1
A3
C2
A2
A1
C3
C4
C5
C6
C7
C8
C9
C12
A4
A5
A6
A7
0 10 20 30km

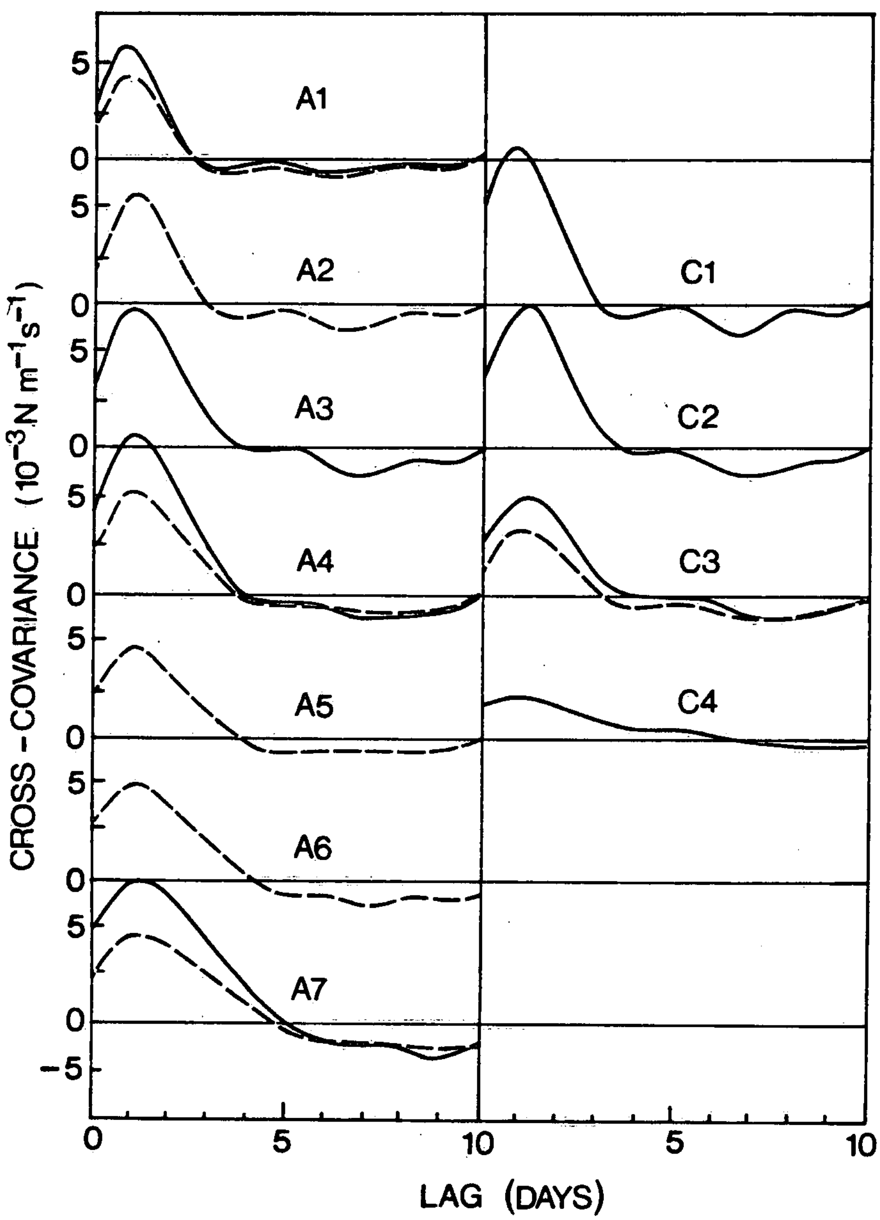
A1
A2
A3
A4
A5
A6
A7
C1
C2
C3
C4
CROSS - COVARIANCE (10^{-3}N $m^{-1}s^{-1}$)
LAG (DAYS)
5
0
-5
10

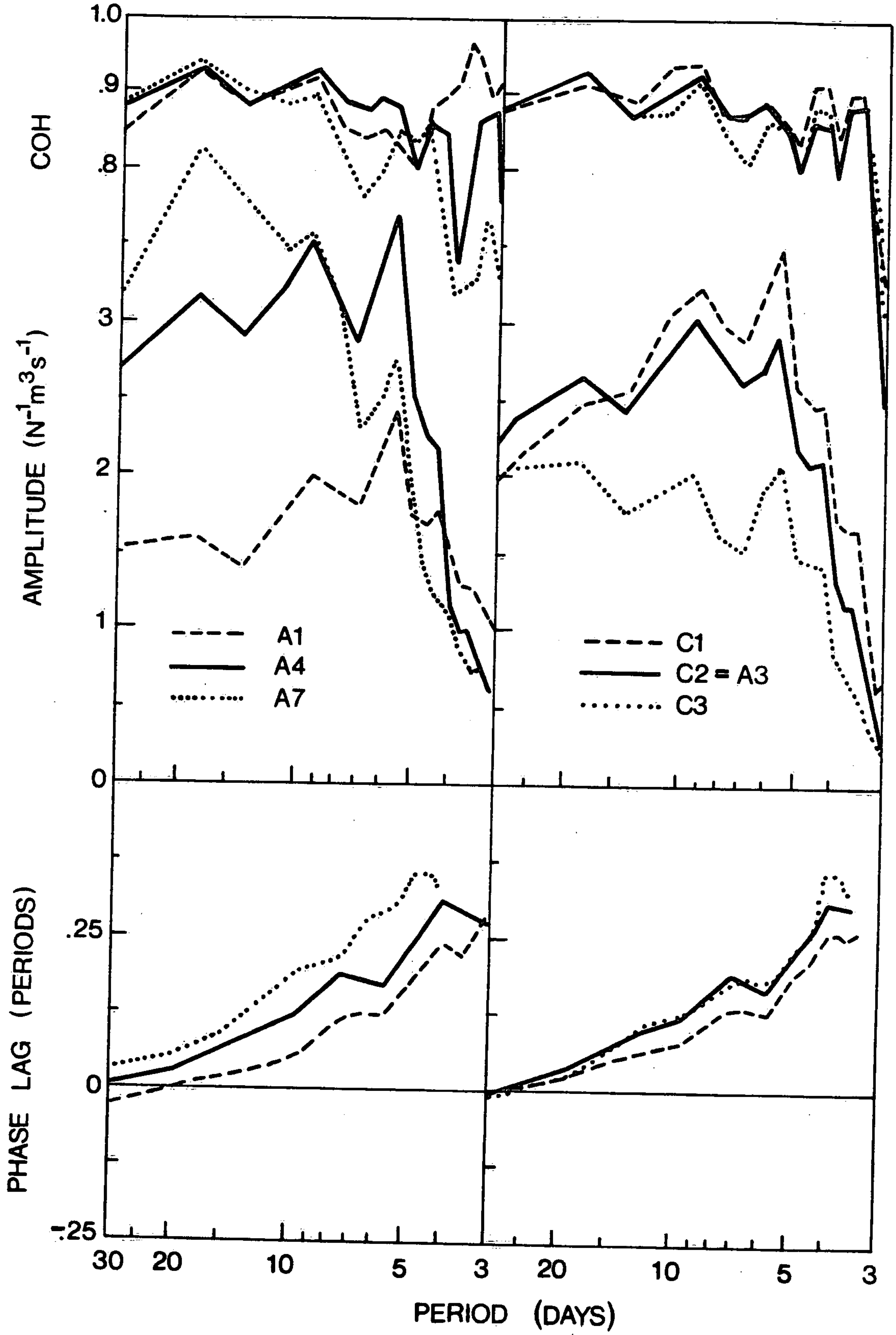

COH
AMPLITUDE ($N^{-1}m^3s^{-1}$)
PHASE LAG (PERIODS)
1.0
.9
.8
3
2
1
0
.25
0
-.25
A1
A4
A7
C1
C2 = A3
C3
30
20
10
5
3
20
10
5
3
PERIOD (DAYS)

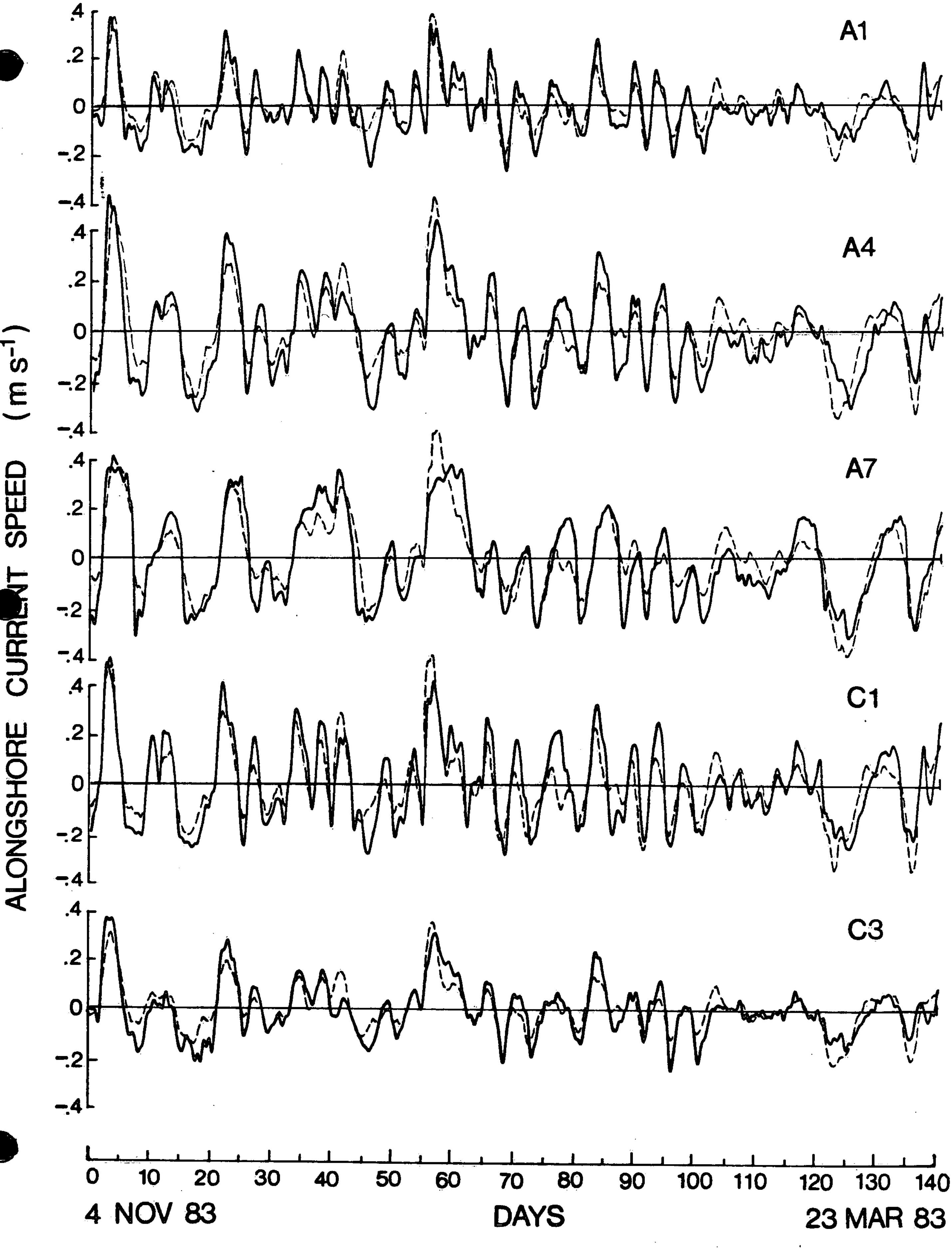
A1
A4
A7
C1
C3
.4
.2
0
-.2
-.4
ALONGSHORE CURRENT SPEED (m s-1)
0 10 20 30 40 50 60 70 80 90 100 110 120 130 140
4 NOV 83
DAYS
23 MAR 83

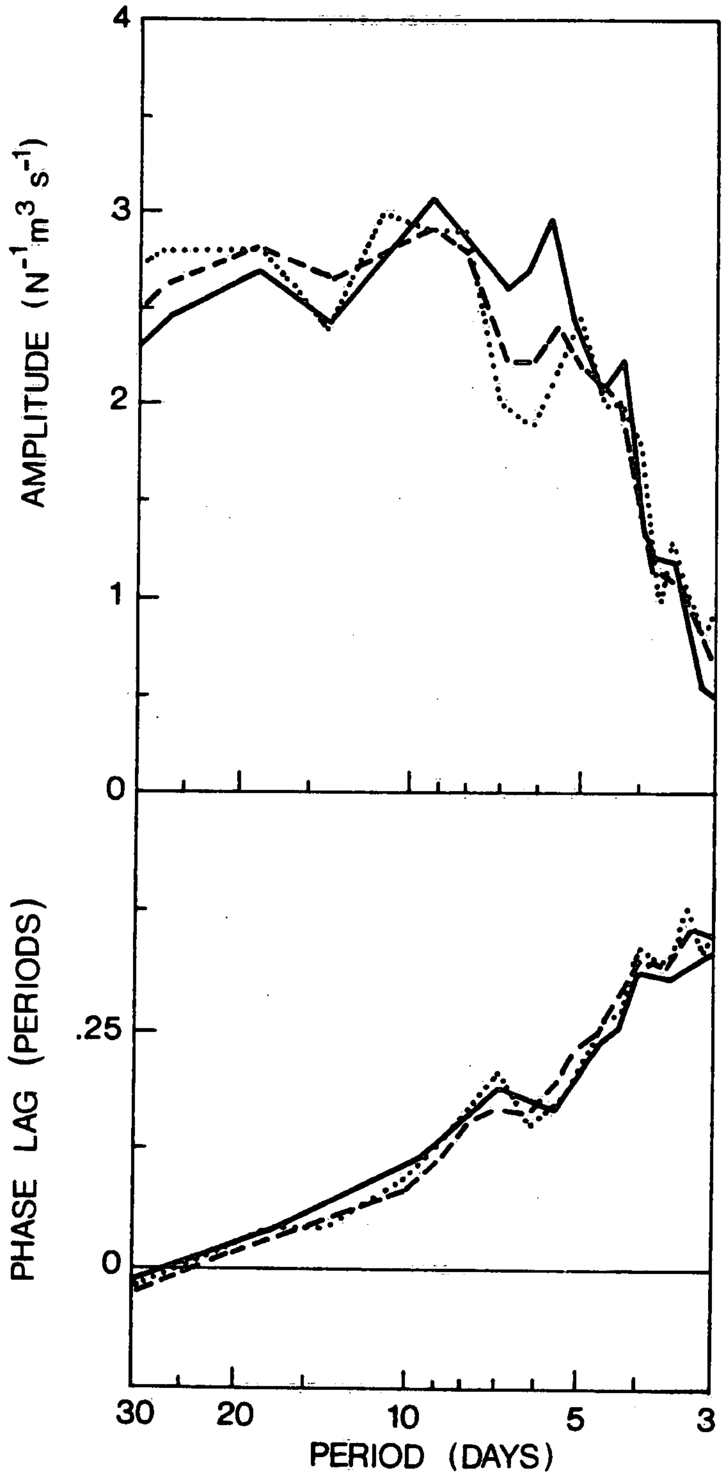

AMPLITUDE $(N^{-1} m^3 s^{-1})$
4
3
2
1
0
PHASE LAG (PERIODS)
.25
0
30
20
10
5
3
PERIOD (DAYS)

9755